Cement and Concrete Research 40 (2010) 1517–1523

Contents lists available at ScienceDirect

Cement and Concrete Research

journal homepage: http://ees.elsevier.com/CEMCON/default.asp

The mini-conical slump flow test: Analysis and numerical study

Adrien Bouvet [a], Elhem Ghorbel [a], Rachid Bennacer [a,b,*]

[a] University de Cergy-Pontoise, L2MGC F-95000 Cergy-Pontoise, France
[b] LMT-ENS Cachan, 61 av. du president Wilson F-94235 Cachan Cedex, France

ARTICLE INFO

Article history:
Received 14 July 2009
Accepted 8 June 2010

Keywords:
Fresh concrete (A)
Rheology (A)
Workability (A)
Cement paste (D)
Modeling (E)

ABSTRACT

This paper provides a general study on cement paste flow. Both mini-slump and Marsh cone tests are used to evaluate the workability of fresh paste mixtures derived from self compacting concretes. A numerical approach is used to reproduce global flow behavior and to check the accuracy of the obtained viscosity as well as the validity of expressions available in the literature giving yield stress from the final diameter of slumped paste. The computational modeling allows access to local information in order to analyze different regions and corresponding flow types, *i.e.* falling solid and flowing fresh cementing material mixtures.
The limitation of some empirical models allowing the prediction of yield stress τ_0 and plastic viscosity μ from mini-slump tests is underlined, conditions of validity are expressed and a new expression is proposed.

1. Introduction

Fresh concretes are constituted by a matrix which is a cement paste and by fine and coarse aggregates. To cast a given element, the concrete must be sufficiently fluid to fill the formwork. Consequently, the concrete design for a specific application and its performances are controlled by its rheological properties. Rheological properties must be evaluated scientifically for real predictability to be achieved. The rheology of concrete is governed by the fluidity and the packing density of the cement paste and by the particle size distribution of the aggregates [1,2]. Some authors [3] considered the matrix as the association of coarse aggregates and mortar which could act as a continuous phase. Nevertheless, the rheology of mortar is partially controlled by the rheology of the cement paste and the properties of the fine aggregates. Although aggregates play an important role on the concrete flow characteristics [4], it can be assumed that any change in the concrete flow properties is, mainly, due to changes in the cement paste rheology. The rheological parameters characterizing the workability of the cement paste are the yield stress "τ_0" which corresponds to the stress required to initiate flow and the plastic viscosity "μ" which describes the paste resistance to flow under external stress. Several models allow to relate these two parameters and to represent the rheological behavior of fresh paste mixtures: the pseudo-plastic model, Bingham or Herschel–Bulkley [5]. The Herschel–Bulkley model, described by Eq. (1), seems to be very effective for cement paste applications.

$$\tau = \tau_0 + \mu\dot{\gamma}^n \quad (1)$$

* Corresponding author. University de Cergy-Pontoise, L2MGC F-95000 Cergy-Pontoise, France. Tel.: 33 (0) 1 34 25 68 86; fax: 33 (0) 1 34 25 68 41.
E-mail address: bennacer@u-cergy.fr (R. Bennacer).

0008-8846/$ – see front matter
doi:10.1016/j.cemconres.2010.06.005

In Eq. (1) τ_0, $\dot{\gamma}$ represent respectively the yield shear stress (Pa) and the shear rate (s^{-1}) while n is a material parameter giving indications on the degree of the fluid dilatancy ($n \succ 1$, the fluid is dilatants and $n \prec 1$ is attributed to pseudo plastic fluid). The Bingham model is recovered for $n=1$ while the Newtonian model is deduced for $n=1$ and $\tau_0=0$. The identified values of these rheological parameters (τ_0, μ) vary according to the used measurement techniques. Different kinds of rheometers are developed in order to quantify rheological behavior of fresh pastes. However, such apparatus are relatively expensive, require a careful experimental procedure and are not practical when they must be used on construction sites. Mini-slump and Marsh cone tests are, then, used to evaluate the workability of fresh paste mixtures. These equipment are widely used throughout the world and were approved as standard techniques to assess the workability of pastes and grouts [6,7]. The simplicity of use of these equipment in construction sites is at the origin of several investigations focusing on the establishment of relationships expressing the yield stress "τ_0" and the plastic viscosity "μ" from the obtained experimental results [8].

The mini-slump test is the most common method for quality control in characterizing the pastes and grouts. The apparatus is a metallic truncated cone opened at both ends and placed on a metallic plate. When vertically lifting the filled cone, the gravity induces the paste to slump down. This phenomenon occurs if the yield stress is exceeded and will stop when the local stress is below such yield stress. Therefore, the slump test observations are related to the yield stress [8]. With the development of self-compacting concretes the slump height value "***S***" is very important and is difficult to be appreciated accurately. On the other hand, for the low yield stresses the viscous forces and inertia will play a significant role in conjunction with gravitational force at the end of slumping as suggested by Saak [9].

Several analytical models have been developed to relate the height slump values to the material yield stress and density by adopting the assumption that the only stress acting on the material is associated with the material's own weight [9–13]. Moreover these authors show that the size and the geometry of the cone do not affect the obtained results. For paste mixtures derived from self compacting concretes (characterized by low yield stress values or low viscosity), Okado et al. [14] proposed Eq. (2) to relate the yield stress to the mini-cone volume "V_c" and to the slumped paste final diameter named the final spread "D_f=***SF***". The developed model is based on the assumption that only the material's own weight is considered and controlling the phenomena.

$$\tau_0 = \frac{225\,g}{4\pi^2}\frac{\rho V_c^2}{D_f^5} \tag{2}$$

where ρ, g, V_c and D_f are: the paste density, the gravity, the conical volume and the final spread diameter respectively.

Roussel et al. [15] showed that the model suggested by Okado et al. [14] (Eq. (2)) does not allow predicting low yield stresses. They propose to improve it by introducing the surface tension effect:

$$\tau_0 = \frac{1}{4}\frac{D_f^2}{V_c}\left(\frac{225}{\pi^2}\frac{g\rho V_c^3}{D_f^7} - \lambda\right) \tag{3}$$

where λ is a coefficient function of both the unknown tested fluid surface tension and contact angle.

More recently Tregger et al. [16] have studied the rheological properties of different paste compositions. They noted that experimental data follow the same trend as Eqs. (2) and (3) but a great disparity is observed between the predicted and the measured values. They explained these discrepancies by the experimental protocol and the rheological parameter range. They suggested a relation between the measured yield stress, from a concentric cylinder rheometer, and the final diameter of slumped paste by a power law fit:

$$\tau_0 = \frac{2.75 \times 10^{-9}}{D_f^{5.81}}. \tag{4}$$

Moreover they showed that the viscosity is related to the final spread time T_f (time required to reach the final mini-slump spread, in seconds). They proposed an expression (Eq. (5)) for determining the plastic viscosity μ based on the knowledge of τ_0 and T_f from mini-slump test, for a given paste mixture,

$$\mu_0 = \tau_0\left(6.41 \times T_f - 1.94\right) \times 10^{-3}. \tag{5}$$

It should be noticed that the prediction of μ depends on the value of τ_0 determined using the previous equations (Eqs. (2), (3) or (4)) which does not give a satisfactory estimation of low yield stresses.

All these previous suggestions and corrections underline the importance of the cement paste dynamic flow behavior. They suggest that the final spread diameter is controlled by both the yield stress and viscosity. In addition the estimation of the yield stress on the basis of the measured values of D_f is not precise. Based on these remarks, another question relating to the used paste volume (Eqs. (2) and (3)) can be raised: what is the effect of the mini-conical height and shape on the final obtained equilibrium D_f?

Domone and Jin [17] previously showed that two empirical tests must be used to determine the rheological parameters: the mini-slump and the Marsh cone tests, but the main question of the expression accuracy and validity remains. Ferraris and de Larrard [18] have tested different paste mixtures using a parallel plate rheometer and empirical tests. They have observed a correlation between final mini-slump spread and the yield stress while the plot of the obtained flow time from Marsh cone test versus the viscosity shows no correlation at all. As a matter of fact, the flow time reflecting the fluidity of the pastes and grouts depends on the viscosity and the yield stress [19].

From these previous works it is obvious that growth weight (ρ and V_c) and yield stress are not enough to characterize such materials. The spread dynamic must be included. Such improvement was proposed by including the final time spread [15]. However the proposed phenomenological correlation is not general as it was deduced from limited observation and do not incorporate the physical aspect and the nonlinear inertia effect.

In the present work we suggest to discuss the validity of Eqs. (2) and (3) and to establish a more general and robust model allowing the prediction of low yield stresses using experimental results coming from empirical tests and numerical simulations. The first section deals with the experimental apparatus and test allowing the identification of the rheological parameters. The second section describes the model and the numerical approach used. It is followed by a section related to the obtained results and to the discussion.

2. Experimental procedure

Different tests were conducted on specimens made from CEM I 52.5N Portland cement, water and CIMFLUID 2002 superplasticizer. The cement pastes are manufactured using a water–cement ratio of 0.37 ($w/c = 0.37$) by weight and two dosages of superplasticizers 0% and 1.15%.

Two experimental procedures are used in this study to estimate the properties of the cement pastes, the mini-conical test in order to estimate the yield stress τ_0 and the Marsh cone test to identify the plastic viscosity μ.

2.1. Mini-conical test

After removing the filled truncated mini-cone (Fig. 1), the material flows until reaching a steady stable state corresponding to a pancake. The resulting final spread diameter of the fresh paste sample is the mean value of two measurements made in two perpendicular directions. The knowledge of the spread diameter D_f allows to have access to an approximation of the yield stress τ_0. The estimation of the yield stress value, τ_0, from Eq. (2) (or (3)) is valid solely under the equation range validity. A movie of the cement–air interface time evolution is also obtained. Such evolution will be considered as the experimental reference to which the numerical result will be compared.

For the considered formulation the calculated yield stresses are summarized in Table 1 and only a few of the extracted interface shape evolution will be presented. A second possible work could concern the comparison between the mini-conical test and rotational rheometer in order to quantify the error on the estimated yield stress. However

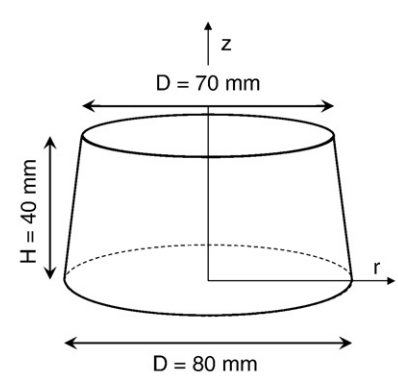

Fig. 1. Schematic view of the considered mini-cone.

Table 1
Cement pastes rheological properties.

	Final spread diameter (mm)	Yield stress τ_0 (Pa) (Eq. (2))	Marsh-conical flow time (s)	Dynamic viscosity μ_0 (Pa s)
Cement paste no. 1	169	20	49.2	1.4
Cement paste no. 2	324	1	22.4	0.6

the results obtained throughout this approach depend strongly on the adopted rheometer geometry (coaxial cylinders; parallel plate, …) and require accurate experimental procedure.

2.2. Marsh-conical test

The Marsh cone is a funnel with a long neck and an opening of 10 mm (see Fig. 2) currently used to determine the required time to a certain amount of cement paste to flow. This experimental procedure allows the estimation of the plastic viscosity μ summarized in Table 1. To assess μ_0, the Bingham model is implemented numerically so that the flow time is estimated and interface shape evolution is monitored. The rheological parameters of Bingham model are τ_0, calculated from Eq. (2) using mini-cone experimental results, and μ which is chosen to allow good agreement between the experimental and numerical flow time. The rheology knowledge will allow us to simulate such material flow and the numerical–experimental comparison will be very helpful in checking the accuracy of such classical test and highlight its validity domain. The obtained local flow phenomena will estimate the inertia effects on the final spread diameter.

3. Model and numerical approach

The considered modeled geometry is represented in Fig. 3. For such geometry and under the assumption of homogeneous cement paste the resulting phenomena will present a vertical axial symmetry. So, by using the cylindrical coordinate a 2-D approach is possible.

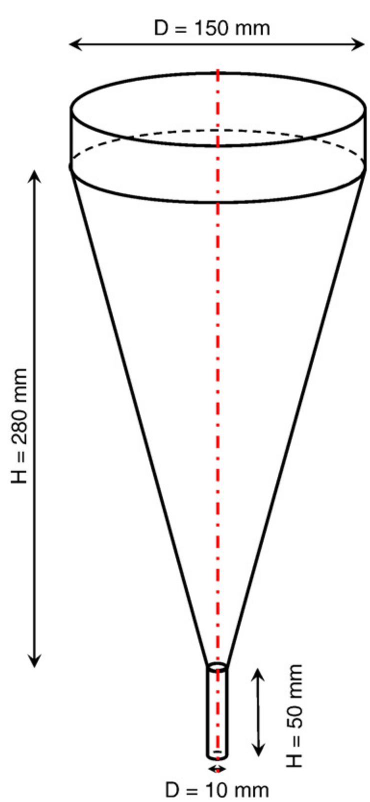

Fig. 2. Schematic view of the considered March cone.

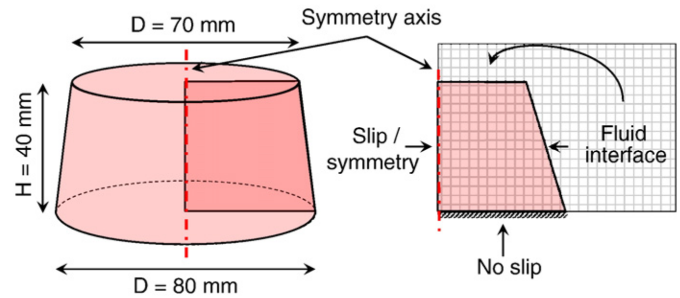

Fig. 3. Computed domain and the boundary conditions.

The flow versus time will be analyzed from the initial trapezoid shape at final state, *i.e.* as initial condition, to the final state.

The shape of the free surface will change during time imposed by the resulting flow. In order to follow such interface change, two different approaches are possible: adaptive mesh or the fixed mesh approach. The first approach is time consuming due to the continuous remeshing domain. Hence, the fixed mesh approach is used in order to avoid such disadvantage. This latter technique is equivalent to that used in enthalpy method in the solid–liquid phase change problem [20]. It consists of a unique computational domain with an equivalent fluid flow. The considered equivalent fluid covering the entire domain exhibit equivalent characteristic (density, viscosity) changing drastically through the interface. The change is implicit as each characteristic is a weighted average of the corresponding properties of the two considered sub-domains (paste and air).

The equivalent characteristic density, ρ, and dynamic viscosity, μ, are given by:

$$\begin{aligned} \rho_{eq} &= \rho_{air}\cdot C + \rho_{grouts}\cdot(1-C) \\ \mu_{eq} &= \mu_{air}\cdot C + \mu_{grouts}\cdot(1-C) \end{aligned} \tag{6}$$

where C represents the air fraction and reaches the value of 1 in the air and 0 in the paste domain.

The flow evolution is governed by the momentum and mass conservation equations:

$$\rho\left(\frac{\partial\vec{V}}{\partial t} + \vec{V}\left(\nabla\vec{V}\right)\right) = \nabla\left[-pI + \mu\left(\nabla\vec{V} + \left(\nabla\vec{V}\right)^T\right)\right] + \rho\cdot\vec{g} \tag{7}$$

$$\frac{\partial\rho}{\partial t} + \nabla\left(\rho\cdot\vec{V}\right) = 0 \tag{8}$$

The tracking interface is possible by considering a scalar transport (Eq. (9)) with a filtering function in order to avoid the numerical diffusion and maintaining a thin interface.

$$\frac{\partial C}{\partial t} + \vec{V}\cdot\nabla C = 0 \tag{9}$$

where $\vec{V}$, p, t and $\vec{g}$ are, respectively, the velocity vector, the pressure, the time and the gravity.

The Bingham rheological model used induces an infinite apparent viscosity when the shear stress is lower than the yield stress threshold τ_0 (Fig. 4). In order to avoid such singularity, several regularization functions are available [21–23]. The Carreau model [22] is, then, used and the equivalent viscosity is given by:

$$\frac{\mu_{equiv}(\dot{\gamma})-\mu_\infty}{(\mu_0-\mu_\infty)} = \left(1 + \left(\frac{\mu_0}{\tau_0}\right)^2\dot{\gamma}^2\right)^{\frac{(n-1)}{2}} \tag{10}$$

where μ_{equ} is the apparent viscosity, μ_∞ is the infinite viscosity corresponding to unlimited shear rate (called plastic viscosity), μ_0 is

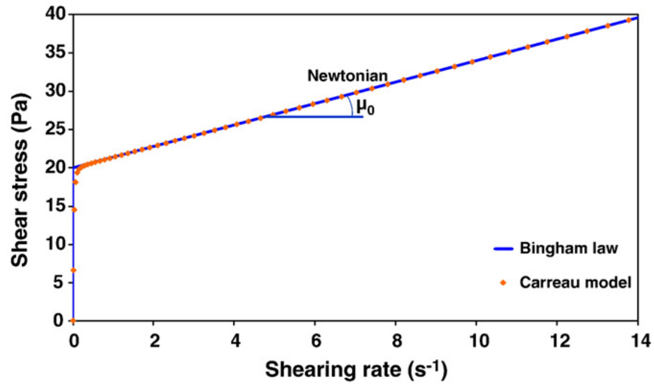

Fig. 4. Shear stress versus shearing rate $\dot{\gamma}$.

the viscosity value corresponding to the zero shear rates and n is the filter controlling parameter. Such a parameter is physically coherent and is generally used to represent a Herschel–Buckley behavior. The higher the μ_0 the better is the approximation but the numerical stability is affected. The adequate and commonly used shear rate in such problems is $\mu_0/\mu_\infty = 500$.

The shear rate γ in a cylindrical case is given by:

$$\dot{\gamma} = \sqrt{2\cdot\left(\left(\frac{\partial u}{\partial r}\right)^2 + \left(\frac{\partial v}{\partial z}\right)^2 + \left(\frac{u}{r}\right)^2\right) + \left(\frac{\partial u}{\partial z} + \frac{\partial v}{\partial r}\right)^2} \qquad (11)$$

where u and v are the r–z velocity components.

4. Results and discussion

The previously presented model was resolved on a fixed grid using a commercial code COMSOL [24]. The set level method allows the interface tracking and the weighting technique makes available the use of a unique equation over the whole domain with an equivalent physical property function of the spatial existence phase (paste or air).

The Portland cement paste rheological properties, previously identified in Section 2 (cement paste no. 1 $\tau_0 = 20$ Pa and $\mu_0 = 1.4$ Pa s), were used to get numerical results. The obtained results are presented in Fig. 5. This figure illustrates the cement paste–air interface displacement over time. The shape is evolving from the initial conical shape to the pancake shape. It is obvious from these numerical results (Fig. 5) that the model allows a description of the dynamic and static effects when cement pastes flow.

The previous recorded experimental interface evolution movie is used to extract a selection of images corresponding to the obtained numerical results. Fig. 6 shows a comparison between experimental and numerical results, the sudden flow appearing and its evolution

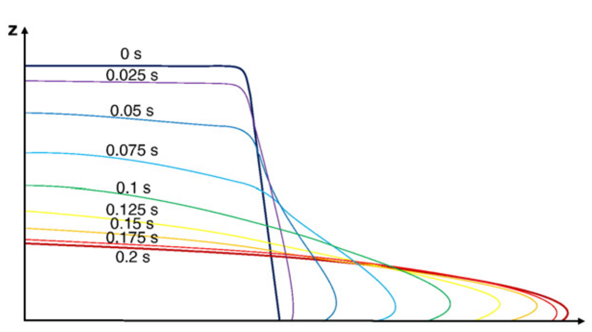

Fig. 5. Example of interface displacement results obtained during the slump flow test (τ_0 = 20 Pa and μ = 1.4 Pa s).

from the conical initial shape to the obtained pancake at the final stage. The global agreement between the numerical and the experimental interface shape evolution during the cement paste flow ensures the validity of the used model. In addition, it allows having local information on the shear stress represented by the isocontours (Fig. 6). This information is useful for the identification of the domains where the cement paste is flowing either as solid or liquid. The analysis of the shear stress isocontours shows that:

- In the middle zone of the mini-cone, close to the vertical symmetrical axe, the cement paste behaves as a Newton fluid and the shear stress values are less than the yield stress ($\tau \prec \tau_0$). No relative displacements are observed in this domain.
- Close to the free surface of the mini-cone and far from the vertical symmetrical axe, the calculated shear stress values are above the yield stress ($\tau \succ \tau_0$) and flow takes place. However, during the flow the shear stress values decrease due to the velocity diminution and tends to the value of the yield stress. Consequently, the flow is stopped when $\tau \prec \tau_0$.

It must be evoked that the rheological parameters τ_0 and μ_0 have been identified from experimental study with relative accuracy due to the used techniques (manual taking off the cone and the possible limitation of the used Eq. (2)). In order to check the precision of the present approach and the related final results versus the rheological parameters, several numerical sensitivity studies are carried out.

The Portland cement paste rheological properties τ_0 and μ variations are considered. The first results, presented in Fig. 7, deal with the sensitivity of the final spread diameter and of the flow time with the Portland cement paste rheological properties. It is noted that ±20% variation of the rheological properties (yield shear stress and viscosity) induces a weak effect on the final spread diameter. Overall yield stress variation of ±20% generates the final diameter variation less than 3%, corresponding to less than 4 mm. As expected, the spread diameter is more important for cement pastes with low yield shear stress. The observed weak effect is a direct consequence of cylindrical evolution where the diameter variation decreases with the increase in pancake size. Moreover, Fig. 7 shows that the flow time is more affected by the variation of the yield shear stress than by that of the viscosity. The observed flow time variation reached about 7% for yield stress while it is less than 2.1% for viscosity change. The required time to reach the final equilibrium state increases with the yield stress while it diminishes when the viscosity of the cement paste enhances.

It must be pointed out that it is difficult to complete the experimental conical test by time recording because the phenomena is fast and the obtained time remains less or of the same order than the time required to lift the cone by the user. So the numerical observations are useful to analyze the dynamic flow resulting from the potential energy stored in the cement paste filling the mini-cone.

The free surface evolution results from pressure difference (original stress) which overcomes locally the yield shear stress on some material regions. The flow takes place on these regions. The obtained flow "Kinetic energy" results from the potential energy and the remaining energy is partly lost in friction and partly stored in cohesion energy (in the final state, where the local stress is below the yield stress on the entire domain).

It can be argued that the main phenomenon controlling the final spread diameter is the yield stress. For very low yield stress, corresponding to liquid material limit, the resulting flow induces a continuous diameter rise; the final spread diameter is reached owing to the surface tension. In the present study the surface tension at the cement paste–air interface is equal to 0.07 Nm^{-1}. This value is dominant in the fluid case but is negligible in the Binghamian fluid with significant yield stress.

Fig. 8 shows the numerically obtained final spread diameter versus different yield stress ($\tau_0 \in [1; 24]$). The Portland cement paste no. 1 (μ_0 = 1.4 Pa s^{-1}) results are represented by circle dots. As expected,

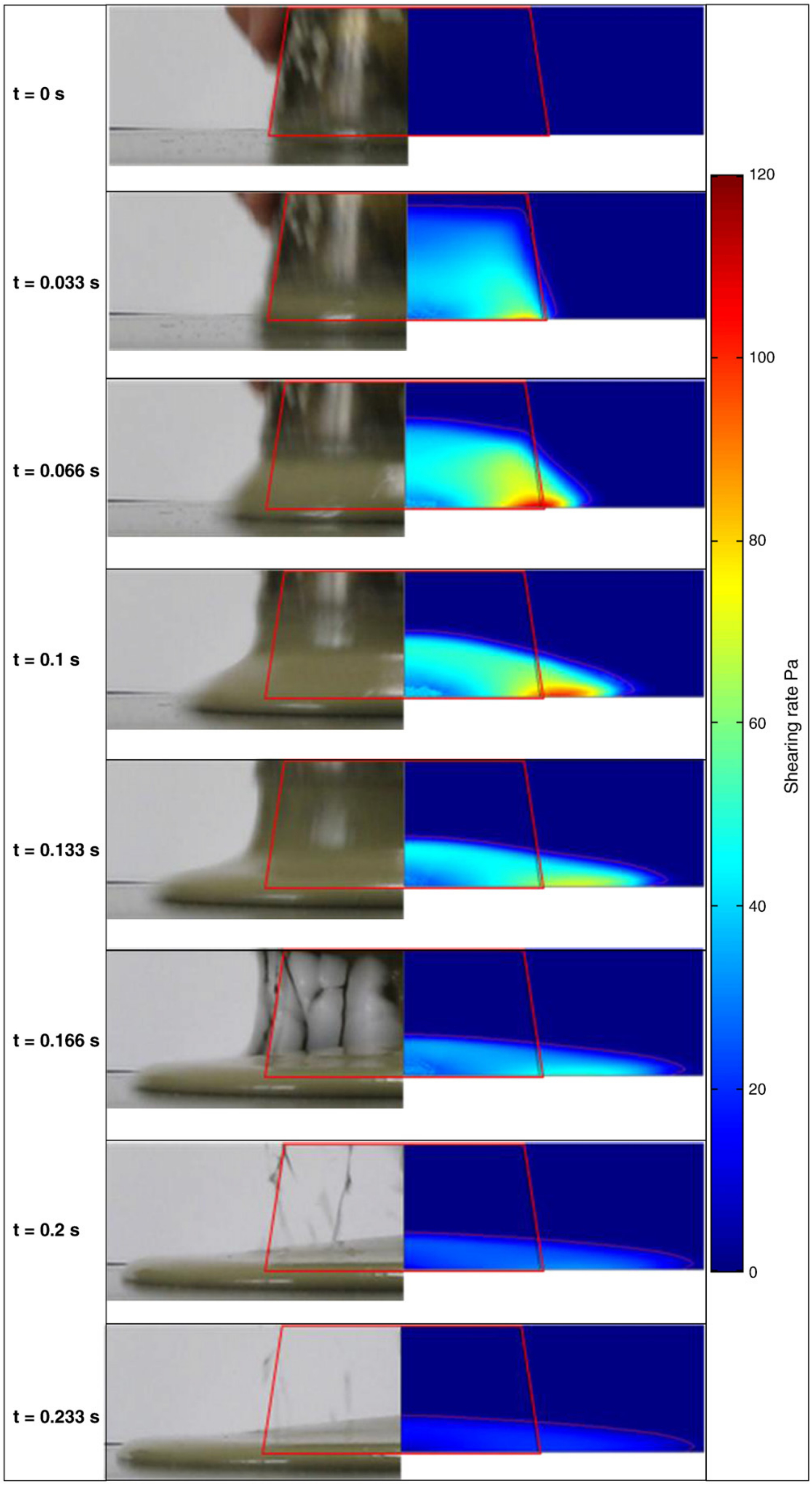

Fig. 6. Comparison between experimental and numerical results.

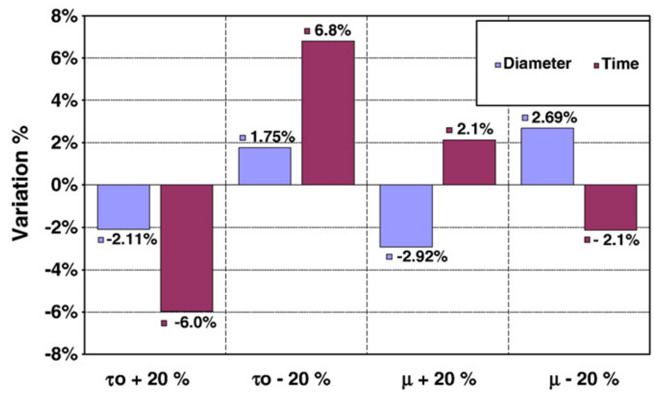

Fig. 7. Results of the rheological properties sensibility test. a) Absolute sensibility and b) relative sensibility.

the final spread diameter decreases when the yield stress increases and it tends asymptotically to the bottom diameter of the cone. However, when the yield stress decreases the cement paste becomes more and more fluid and the final spread diameter raises an asymptotic value resulting from the relative weight of the surface tension and gravity.

The evolution of the D_f versus τ_0 is quite linear (while neglecting inertia and surface tension effect) for yield shear stress higher than 8 Pa (Fig. 8). The results obtained using Eq. (2) are represented by a dashed blue line and compared to the obtained numerical spread diameter. Good agreement is observed for yield stresses higher than 20 Pa. In this case, the values of the final spread diameters are very close. Moreover they are subjected to experimental errors. For instance, a diameter variation of 1 cm causes a significant change in the yield shear stress (20 to 40 Pa).

A disparity is observed between the predicted using Eq. (2) and the numerical spread diameter values for low yield stresses (Fig. 8). The model proposed by Roussel (Eq. (3)) taking into account surface tension effects improves the predicted results for a wide range of yield stresses. However both models (Eqs. (2) and (3)), represent a first approach to estimate the yield stress, an approach that does not include the dynamic effects which are significant for fluid cement pastes characterized by low yield stresses. The related viscosity of cement pastes, which flow evolution is described in Fig. 8 using Eq. (3), corresponds to $\mu_0 \cong 1.5$ Pa s. The importance to introduce in cement paste flow modeling the dynamic effects is illustrated by the numerical and experimental results obtained for the Portland cement paste no. 2 corresponding to the following rheological properties

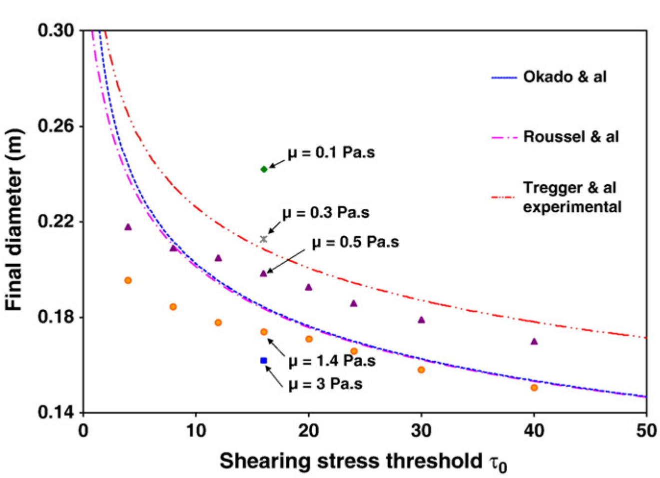

Fig. 8. Evolution of the final diameter according to the yield shear stress.

Table 2
Geometrical characteristics of the used mini-cones.

	1	Base	2
H (mm)	50	40	30
$Radius_{top}$ (mm)	31.3	35	40.4
$Radius_{bottom}$ (mm)	35.8	40	46.2
V_c (cm^3)	176.9	176.9	176.9
D_f (mm)	164	170	175.6

$\mu_0 = 0.5$ Pa s. The admixture no. 2 is less viscous than the previously analyzed one. The obtained results are represented on Fig. 8 by triangle dots. The spread diameter versus yield stress behavior is the same as that obtained for the first Portland cement paste. The obtained curve corresponds to a sliding effect to a higher diameter value consequence of a more fluid material (less viscous). Such results illustrate clearly the limitation of the classical expression to evaluate the yield stress. The dynamic effect resulting from the fluidity modifies significantly the final spread diameter which became a consequence of both the flow and the yield stress. So the classical approach based on static expression became inadequate. Such limitation is clearly illustrated by some of the obtained numerical results for fixed yield stress and different viscosity (from 0.1 to 3 Pa s). It can be highlighted that the spread diameter increases by decreasing the viscosity of the cement paste which fluidity rises. The dynamic result will overcome the yield stress effect and the final spread diameter will be a direct consequence of the generated dynamic and surface tension in addition to the yield stress. It is also obvious that for high viscosity the spread diameter tends asymptotically to the initial value of the bottom of the mini-cone. At the light of these results it can be concluded that the final spread diameter increases with the decrease of viscosity. Consequently, a new expression (Eq. (12)) is proposed to describe the relation between the spread diameter and the rheological parameters of the cement pastes (τ_0, μ_0).

$$\frac{D_f}{D_f^{ref}} = 1 - \ln\left(\frac{\mu_{equ}}{\mu_0}\right) \times 0.13 \quad \text{where} \quad \tau_0 = \frac{1}{4}\frac{\left(D_f^{ref}\right)^2}{V_c}\left(\frac{225}{\pi^2}\frac{g\rho V_c^3}{\left(D_f^{ref}\right)^7} - \lambda\right) \tag{12}$$

where D_f^{ref} is the reference spread diameter and μ_{equ} is the equivalent viscosity given by Eq. (10).

All the expressions (Eqs. (2), (3) and (12)) relating to the spread diameter to yield shear stress introduce the cone volume and do not take into account the effect of the cone geometrical characteristics. Hence, calculations are carried out using the proposed expression (Eq. (12)) and the following rheological characteristics ($\tau_0 = 20$ Pa and $\mu_0 = 1.4$ Pa s) to investigate the effect of cone geometrical parameters on the final spread diameter (Table 2).

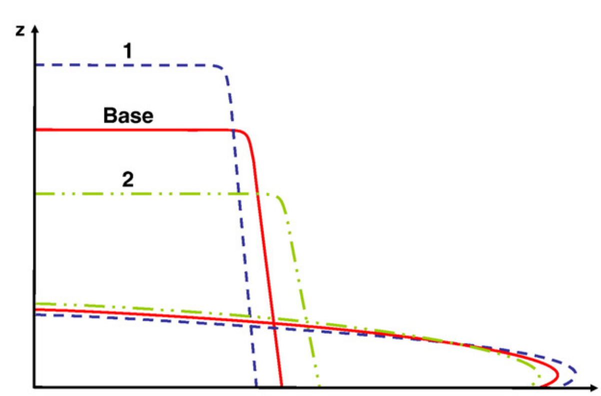

Fig. 9. Results of the sensibility test at the geometrical cone properties.

The three considered cones have the same volume, V_c, and the same top radius/bottom radius ratio. The first one corresponds to the cone analyzed in the previous section. The different conical shapes and the corresponding results are summarized and represented on Fig. 9 (corresponding to the initial state). The results confirm that the increase in the height cone affects the final diameter and induces bigger D_f. These new results suggest a possible solution for the previously underlined asymptotical diameter obtained for materials with relatively high τ_0. In such a situation of a nonsensitive final diameter (Fig. 9) a more slender cone shape is used in order to allow more dynamic effects inducing bigger spread diameter. The solution corresponds to a horizontal sliding of the sensitive region of the observed curve diameter versus yield stress.

5. Conclusion

The present work provides a general study on the paste flow. It focuses on the characterization of Portland cement paste rheological properties. Experiments are conducted in order to well define the viscous character and to get the global Portland Cement Paste flow ability. The numerical approach is used to reproduce the global flow behavior and to ensure the accuracy of the obtained viscosity. The computational modeling permits the access to local information in order to analyze the different regions and the corresponding flow types, *i.e.* falling solid and flowing fresh cementitious materials for concrete.

The experimental results, achieved for Portland cement paste no. 1, describe well the dynamic behavior of the analyzed product and the numerical simulations fit well the experimental results. The agreement between numerical and experimental results is valid only for relatively significant yield stress values and an insignificant fluid growth. The obtained numerical results allow a better understanding of local and global flow, highlight the validity domain of the expression given by Eq. (2) and confirm the need to introduce the surface tension effects for low yield stresses as illustrated in Eq. (3).

The most relevant results can be summarized as follows:

- Below a yield stress of 4 Pa, the final radius is almost constant. In this zone it is the surface stress which constrained the flow.
- When the yield stress is higher than 4 Pa, the final diameter decreases with yield stress increases. The evolution is relatively linear and tends toward an asymptotic value.
- For yield stress higher than 20 Pa the evolution of final spread diameter versus yield stress is very slow, so a small error on the diameter will induce an important change in the estimated yield stress.
- The classical expressions (Eqs. (2) and (3)) became inadequate for low viscosity (more fluid Portland Cement Pastes) due to the significant diameter increase and the important dynamic effects. The resulting diameter is not solely due to the yield stress and the material's own weight but includes dynamic flow.
- A new expression of the final spread diameter D_f as a function of the viscosity is proposed (Eq. (12))
- The influence of the cone shape on the final spread diameter, D_f, is quantified. For a constant Portland cement paste volume, increasing the height of the cone leads to an increase of D_f. Consequently it is easier to measure the final spread diameter for materials with high yield stress, τ_0.

References

[1] A.W. Saak, H.M. Jennings, S.P. Shah, New methodology for designing self-compacting concrete, ACI Materials Journal 98 (6) (2001) 429–439.
[2] F. Mahaut, S. Mokéddem, X.N. Chateau, N. Roussel, G. Ovarlez, Effect of coarse particle volume fraction on the yield stress and thixotropy of cementitious materials, Cement and Concrete Research 38 (11) (2008) 1276–1285.
[3] R.J. Flatt, N. Martys, L. Bergström, The rheology of cementitious materials, Materials Research Society, MRS Bulletin 29 (5) (2004) 314–318.
[4] L. Zhuguo, State of workability design technology for fresh concrete in Japan, Cement and Concrete Research 37 (9) (2007) 1308–1320.
[5] F. de Larrard, C.F. Ferraris, T. Sedran, Fresh concrete: a Herschel–Bulkley material, Materials and Structures 31 (1998) 494–498.
[6] C.F. Ferraris, O.H. Karthik, R. Hill, The influence of mineral admixtures on the rheology of cement paste and concrete, Cement and Concrete Research 31 (2) (2001) 245–255.
[7] M. Şahmaran, N. Özkan, S.B. Keskin, B. Uzal, İ.Ö. Yaman, T.K. Erdem, Evaluation of natural zeolite as a viscosity-modifying agent for cement-based Portland Cement pastes, Cement and Concrete Research 38 (7) (2008) 930–937.
[8] J.E. Wallevik, Relationship between the Bingham parameters and slump, Cement and Concrete Research 36 (7) (2006) 1214–1221.
[9] A.W. Saak, H.M. Jennings, S.P. Shah, A generalized approach for the determination of yield stress by slump and slump flow, Cement and Concrete Research 34 (3) (2004) 363–371.
[10] J. Murata, Flow and deformation of fresh concrete, Materials and Structures 17 (1984) 117–129.
[11] W.R. Schowalter, G. Christensen, Toward a rationalization of the slump test for fresh concrete: comparisons of calculations and experiments, Journal of Rheology 42 (4) (1998) 865–870.
[12] N. Pashias, D.V. Boger, J. Summers, D.J. Glenister, A fifty cent rheometer for yield stress measurement, Journal of Rheology 40 (6) (1996) 1179–1189.
[13] S. Clayton, T.G. Grice, D.V. Boger, Analysis of the slump test for on-site yield stress measurement of mineral suspensions, International Journal of Mineral Processing 70 (1–4) (2003) 3–21.
[14] T. Okado, T. Miyagawa, Study on a method of obtaining rheological coefficients of high-flow concrete from slump flow test, Journal of Materials, Concrete Structures and Pavements of JSCE (1999) 113–130 (in Japanese).
[15] N. Roussel, P. Coussot, Fifty-cent rheometer for yield stress measurements: from slump to spreading flow, Journal of Rheology 49 (3) (2005) 705–718.
[16] N. Tregger, L. Ferrara, S.P. Shah, Identifying viscosity of cement paste from mini-slump-flow test, ACI Materials Journal 105 (6) (2008) 558–566.
[17] P.J. Domone, J. Jin, Properties of mortar for self compacting concrete, Proc of First Int. Rilem Symp. On Self Compacting Concrete, SARL, RILEM, 1999, pp. 109–120.
[18] C.F. Ferraris, F. de Larrard, Testing and Modelling of Fresh Concrete Rheology, NISTIR, 1998, p. 6094.
[19] N. Roussel, R. Le Roy, The marsh cone: a test or a rheological apparatus? Cement and Concrete Research 35 (5) (2005) 823–830.
[20] R. Bennacer, M. El Ganaoui, El. Semma, Quelques paramètres de contrôle de la convection thermocapillaire en croissance par fusion de zone en microgravité, Comptes Rendus Mecanique 332 (5–6) (2004) 447–456.
[21] M.M. Cross, Rheology of non-Newtonian fluids: a new flow equation for pseudoplastic systems, Journal of Colloid Science 20 (1965) 417–437.
[22] P.J. Carreau, Rheological equations from molecular network theories, Trans. Soc. Rheol. 16 (1972) 99–127.
[23] K. Yasuda, Ph. D. thesis, Massachusetts Institute of Technology, 1979.
[24] COMSOL Multiphysics Finite Element Analysis Software, Tutorial-site http://www.comsol.com/.